EVOLUTION & DEVELOPMENT 11:4, 422–433 (2009)
DOI: 10.1111/j.1525-142X.2009.00348.x

Heterochronic shifts explain variations in a sequentially developing repeated pattern: palatal ridges of muroid rodents

Sophie Pantalacci,* Marie Sémon, Arnaud Martin, Pascale Chevret, and Vincent Laudet

Institut de Génomique Fonctionnelle de Lyon, Université de Lyon, Université Lyon 1, CNRS, INRA, Ecole Normale Supérieure de Lyon, 46 allée d'Italie, 69364 Lyon Cedex 07, France

*Author for correspondence (email: sophie.pantalacci@ens-lyon.fr)

SUMMARY Metazoans are largely made of repeated parts, and metazoan evolution is marked by changes in the number of these parts, called meristic evolution. Understanding the mechanisms associated with meristic changes is thus a critical issue to evolutionary developmental biology. Palatal rugae are sensory ridges regularly arranged on the hard palate of mammals. They develop sequentially following mesio-distal growth of the palate, and activation–inhibition mechanisms very likely control spacing and timing of this sequential addition. In this study, we characterized trends in rugae number evolution among muroid rodents, showing that most species display 8 ± 1 rugae, changes by one being very frequent in the phylogeny. We then compared development of three muroid species: mouse (nine rugae), rat (eight), and golden hamster (seven). We showed that palatal growth rate, spacing, and addition rate in mouse/rat were remarkably similar (with respect to the embryo size difference), and that increase to nine rugae in mouse is achieved by postponing the end of the addition process (hypermorphosis). Such a heterochronic shift may be typical of ± 1 variations observed among muroid rodents. In contrast, decrease to seven rugae in golden hamster is attributed to early growth termination (progenesis) of the palate, which correlates with the severe shortening of gestation in this species. Our results provide an experimental support to the intuitive view that heterochronies are especially relevant to meristic evolution of traits that rely on a sequential addition process. We also interpret our results in the light of developmental constraints specifically linked to this kind of process.

INTRODUCTION

Metazoans are largely built of repeated parts, and, as pointed out by Rudolf A. Raff (1996), "Meristic changes, that is, alterations in numbers of a standard part, are one of the most common occurrences in evolution," another one being the differentiation of these parts from the standard. Understanding how these meristic changes occur is thus a critical issue to understand the evolution of forms.

Different types of developmental mechanisms underlie these repeated patterns and may confer them different evolutionary properties. For example, an important distinction is whether they arise in a simultaneous or sequential manner. Examples of simultaneously emerging patterns are the segments of short band insects like *Drosophila*, the microchaetes, and trichomes of arthropods epidermis, the primary hair follicles in mammals, the ocelli of butterfly wings, and the spreading patterns of feather follicles and scales. In contrast, sequentially emerging patterns rely on a tight coupling with tissue growth where pattern addition is concomitant with liberation of new space by cell proliferation. The segments of most arthropods and annelids, the somites of vertebrates, the digits and phalanges of tetrapods, and the molars of mammals are examples of structures that follow a sequential addition mode of development. In theory, changes in the timing (heterochronies) of the sequential addition process can explain meristic variation, by changing the pace of patterning and by modulating the duration of the process. A slower/shorter patterning process will decrease the number of structures (leading to paedomorphosis), while a faster/longer patterning process will increase it (leading to peramorphosis). (For more about heterochronies and associated vocabulary see [Raff and Wray 1989; Raff 1996; McNamara 1997; Smith 2002, 2003].) Despite its simplicity and its impact on our understanding of meristic evolution, relatively little developmental data have documented this theoretical framework. Gomez et al. 2008 recently showed that the drastic increase of snakes somite number is achieved through a combination of a slower growing presomitic mesoderm (the growth zone from which somites are laid down) with longer lifespan and a faster ticking segmentation clock compared with other vertebrates. Heterochronies were also proposed to explain the derived number of segments in Chaetopterid annelids (Irvine et al. 1999), hypodactyly of the lizard *Hemiergis* (Shapiro et al. 2003) and,

hyperphalangy in the spotted dolphin (Richardson and Oelschlager 2002).

Palatal rugae provide a nice model to study the development and evolution of repeated structures. Rugae are transversal ridges regularly arranged on the hard palate of mammalian species, and harboring various types of intra-epithelial sensory structures (such as Merckel cells, corpuscular endings, and free nerve endings; Nunzi et al. 2004). During mastication and together with the tongue, rugae thus play a sensory role, but very likely also a mechanical role: they assist the tongue in keeping the mouthful in place during mastication (Eisentraut 1976; Halata et al. 1999; Ishizaki et al. 2006).

In a previous study, we have shown that mouse palatal rugae form sequentially following mesio-distal growth of the secondary palate (Pantalacci et al. 2008). Moreover, analyses of perturbations of the rugae pattern in mutant mice showed that sequential addition of new rugae was only possible at a threshold distance from previously formed rugae, suggesting that activation–inhibition mechanisms may be at work (as is the case for hair and feather follicle spacing) but conditional on the growth of the palate.

Among mammals, rugae are found in definite number, very often between 8 and 10, but rising to more than 20 in some species (especially among artiodactyls), and being very degenerated (e.g., in humans) or even lost in a few cases (e.g., in dolphins where teeth have a seizing more than masticating function, or in whales where rugae may have been transformed to whalebone) (Eisentraut 1976).

Muroid rodents (Muroidea) are the most successful suborder of mammals, representing almost 30% of described placental species, with a main radiation situated about 25 Ma (Steppan et al. 2004). They provide a unique opportunity to study rugae number evolution at a moderate taxonomic scale, while having access to developmental data, because three laboratory species (mouse, rat, and hamster) are muroid rodents.

In this study, we first reconstructed the history of rugae number among muroid rodents to see how rugae number evolved during the diversification of this group. Because the three muroid lab species display different rugae number, we then compared rugae development in these three species to identify the process underlying their meristic variations.

MATERIALS AND METHODS

Reconstructing "rugae number" character history in muroid rodents

Most rugae number data were collected from the literature (Eisentraut 1976, 1981; Lecompte et al. 2002) and for a few cases, directly from specimens kindly provided by F. Catzeflis, S. Renaud, J. Britton (for details, see Table S1).

Molecular phylogeny

We obtained sequences from three nuclear genes (*IRBP*, *GHR*, and *RAG1*) and one mitochondrial gene (*Cytochrome b*) for 74 taxa including representatives of 54 muroid genera and two dipodoid outgroup species. Most sequences were retrieved from Genbank. Three new *IRBP* sequences were sequenced, using the method of Poux and Douzery 2004, and deposited in the EMBL data bank (see Table S1 for all accession numbers). Sequences were manually aligned with Seaview (Galtier et al. 1996), nonsequenced positions and gaps were coded as missing data. Phylogenetic reconstructions were performed on the complete DNA data set by maximum likelihood (ML) with Phyml (Guindon and Gascuel 2003) and by Bayesian inference with MrBayes (version 3.1.2) (Huelsenbeck and Ronquist 2001). Modeltest 3.7 (Posada and Crandall 1998) was used to determine the sequence evolution model that best fitted our data using the Akaike Information Criterion (AIC). In our case, it proved to be the GTR+Γ+I model. The robustness of nodes was estimated in Phyml with ML bootstrap percentages (BP_{ML}) estimated from 1000 pseudoreplicates (Fig. S1). We also performed Bayesian Inference, as calculated by MrBayes, and report Posterior Probabilities (PP; 5,000,000 generations, sampled every 100th, burning = 5000 trees) (Fig. S1). For the Bayesian analysis we used 12 partitions, one for each codon position of each gene.

Character evolution/character states reconstruction

The ancestral states of rugae number were reconstructed by ML using the methods implemented in the BayesMultiStates package (BayesTraits software, available from http://www.evolution.rdg.ac.uk (Pagel et al. 2004). The best model proved to be the simplest model constraining every transition rates between any number of rugae to be equal.

Harvesting and staging of embryos

CD1 (ICR) adult mice were purchased from Charles River. Females were mated overnight (night at 08:00 PM), and, if a vaginal plug was detected in the morning, noon was indicated as embryonic day (ED) 0.5. Other females were kept in a light–dark reversed cycle (night at 12:00 PM), so that the next day at 04:00 PM was considered as ED1.0. Pregnant rat females (*Rattus norvegicus*, CD) were purchased from Charles River. Matings were either overnight (with night at 06:00 PM; noon after morning detection of vaginal plug = ED0.5) or between 7:00 AM and 11:00 AM in the morning (noon after detection of vaginal plug = ED0). Pregnant hamster females (*Mesocricetus auratus*, HsdHan:AURA) were purchased from Harlan (matings from 03:00 to 06:00 PM, following afternoon at 03:00 PM = ED1.0).

Pregnant mice were killed by cervical dislocation, rats by carbon dioxide inhalation, and hamsters by cervical dislocation following anesthesia. Mouse, rat, and hamster embryos were harvested and weighted as described for mouse embryos (Peterka et al. 2002).

Whole mount in situ hybridization

In situ hybridization was performed using standard methods (Hogan et al. 1994) on previously dissected embryonic upper jaws. Mouse and hamster *Shh* probes were as described in Pantalacci et al. 2008. The rat *Shh* probe was made from reverse transcriptase-polymerase chain reaction (RT-PCR) products amplified from rat

embryonic total RNA and cloned in TOPO-PCRII (Invitrogen, Carlsbad, CA, USA) with the following primers: 5′ ATGGAA CACCCSCTCTTTGG and 3′ CCACACTTTCACCTGTCTT TCAGT.

Imaging, measures, and statistical analysis

Samples were imaged on a LUMAR stereomicroscope (Zeiss, PLATIM, Lyon). All measures were performed with the program Axiovision. The distance between two rugae was determined as the distance between the midline of *Shh* stripes (embryos) or rugae (adults) along a virtual line cutting the hemi palate in two equal parts. Statistical and graphical analysis were performed using R (Team 2008, http://www.R-project.org).

Weight to time conversion

We collected information on rough ED (estimated according to above mating protocols) and weight class for 821 mouse embryos (corresponding to more than 65 litters) and 246 rat embryos (21 litters). From these data, we represented weight (mg) as a function of time (days) for each species (Fig. S2).

For hamster (6 litters), we had inconsistencies between weight or developmental stage as estimated from embryo features and the supposed age of the litter according to mating dates. Comparison with published data (Lee et al. 1975) suggested two litters for which the age of gestation had obviously been overestimated (Fig. S2). Because other litters matched published data, we used these data to represent weight as a function of time for this species (Fig. S2).

In the three species, this weight to time relationship could be adequately linearized for the time period of interest when using ln of weight (Fig. S2). We found ln (weight) = 0.52 × time − 1.88 ($R = 0.95$) for mouse; ln (weight) = 0.57 × time − 3.02 ($R = 0.95$) for rat; and ln (weight) = 0.81 × time − 4.25 ($R = 0.98$) for hamster. We then deduced the reverse linear relationship time = f (ln weight) to estimate for each embryo a precise age from its weight.

Comparison of developmental rates

Mouse, rat, and hamster development were compared based on published detailed studies (respectively, Boyer 1948; Altman 1962; Theiler 1972). We performed two by two comparisons: mouse–hamster, based on Theiler staging, and rat–hamster, based on Witschi staging (Fig. S3). This provided an indirect comparison of mouse and rat development, which were found to be parallel, in agreement with comparisons made by other authors (Altman 1962; Monie 1976). This indicated the validity of our mouse–hamster and rat–hamster comparisons.

RESULTS AND DISCUSSION

Evolutionary history of rugae number in muroid rodents

In order to study the evolutionary history of rugae number, we collected data on rugae number (mainly from the extensive work of Eisentraut 1976, 1981) and reconstructed a molecular ML phylogeny for the concerned taxa (see "Materials and methods" for details and Fig. S1 for the phylogeny). Based on this phylogeny, which was congruent with published phylogenies (Jansa and Weksler 2004; Steppan, Adkins, and Anderson 2004; Lecompte et al. 2008), we inferred the history of variations in rugae number using BayesTraits (see "Materials and methods").

According to this reconstruction, the common ancestor to all muroid rodents likely had seven or eight rugae (respectively, red and orange in Fig. 1A; seven being more likely with $P = 0.63$ vs. 0.28), and the common ancestor of the next radiation (including Muridae, Cricetidae, and Nesomyidae) had eight rugae ($P = 0.99$). Most rodents in these three groups kept eight rugae, but frequent changes are observed: decreases to seven rugae (red, at least six independent cases) or increases to nine rugae (yellow, at least four independent cases) (see also some patterns documented on Fig. 1B). Some species seem to be polymorphic with eight or nine rugae (at least five cases), as seen, for example, in the *Mus musculus* CD1 lab strain (Fig. 1B). More drastic changes are, however, rare: we observed an increase up to 10 rugae in the *Praomys* group (green, see also Fig. 1B), an increase up to 12 rugae in *Batomys* (light blue on Fig. 1A) and two independent cases of even more radical increases: *Phloeomys* (a sister genus to *Batomys*) had more than 20 rugae (purple in Fig. 1A) and *Uromys* had 15 rugae (dark blue in Fig. 1A). Of note, in these species, large, spaced rugae face the diastema as in any other species, while narrow, closely packed rugae are observed in the intermolar area (Fig. 1B).

In summary, based on the reconstruction, we observed frequent, independent minor variations (± 1 ruga) relative to the standard state, that is eight rugae, with more drastic variations in only two independent lineages: within the Phloeomyini (*Phloeomys, Batomys*) and within Hydromyini (*Uromys*).

Three muroid species easily available for lab experiments display different rugae number. The rat *R. norvegicus* displays

Fig. 1. Evolutionary variations in rugae number and pattern among muroid rodents. (A). History of rugae number evolution in muroid rodents as reconstructed using BayesTraits and a maximum likelihood phylogeny. Character state (rugae number) is symbolized with colored pies at the tip of each branch (pies with two colors represent possible polymorphism in a particular species). The probabilities for each ancestral state are symbolized for each node with a colored pie. For full species name and phylogeny support, see Fig. S1. (B) Pictures and drawings illustrating variations in rugae number among muroid rodents pointed in (A) Rugae number is indicated in the corner for each species. Picture of *Oecomys* is courtesy of F. Catzeflis. Other pictures were made on specimens kindly provided by S. Renaud, J. Britton, and S. Riebel-Foisset, except for *Mus musculus* and *Mesocricetus auratus* lab specimens. Drawings were performed on original pictures or drawings by Eisentraut (1976, 1981). Scales are mentioned when available.

the ancestral number, that is eight rugae. As mentioned earlier, mice of the CD1 strain represent a case of increase by one, because they tend to have nine rugae (half of the individuals, Fig. 1B). Finally, the hamster *M. auratus* represents a case of decrease by one, because it has only seven rugae (Fig 1B). Hence we could investigate the nature of the developmental differences between these three species.

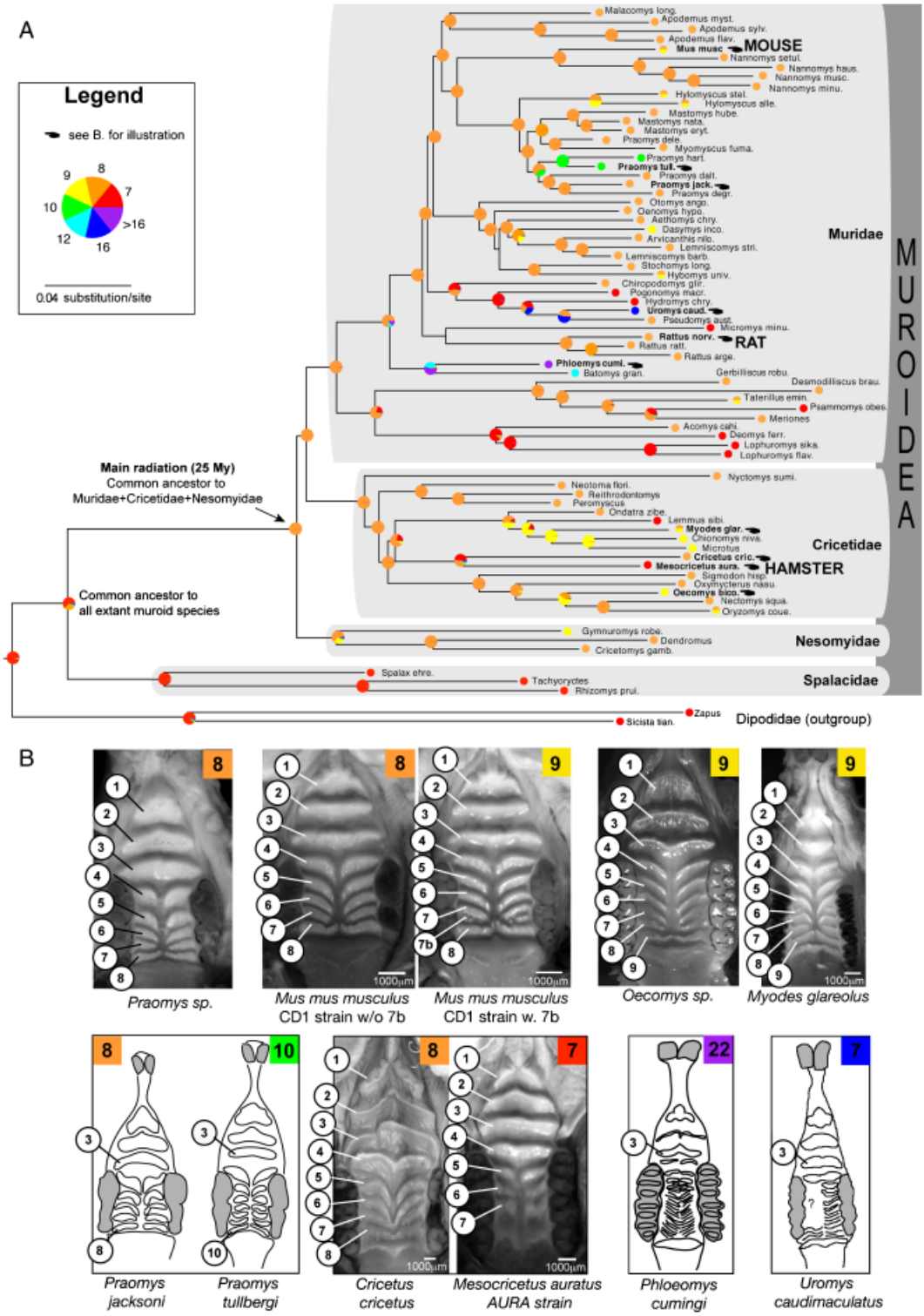

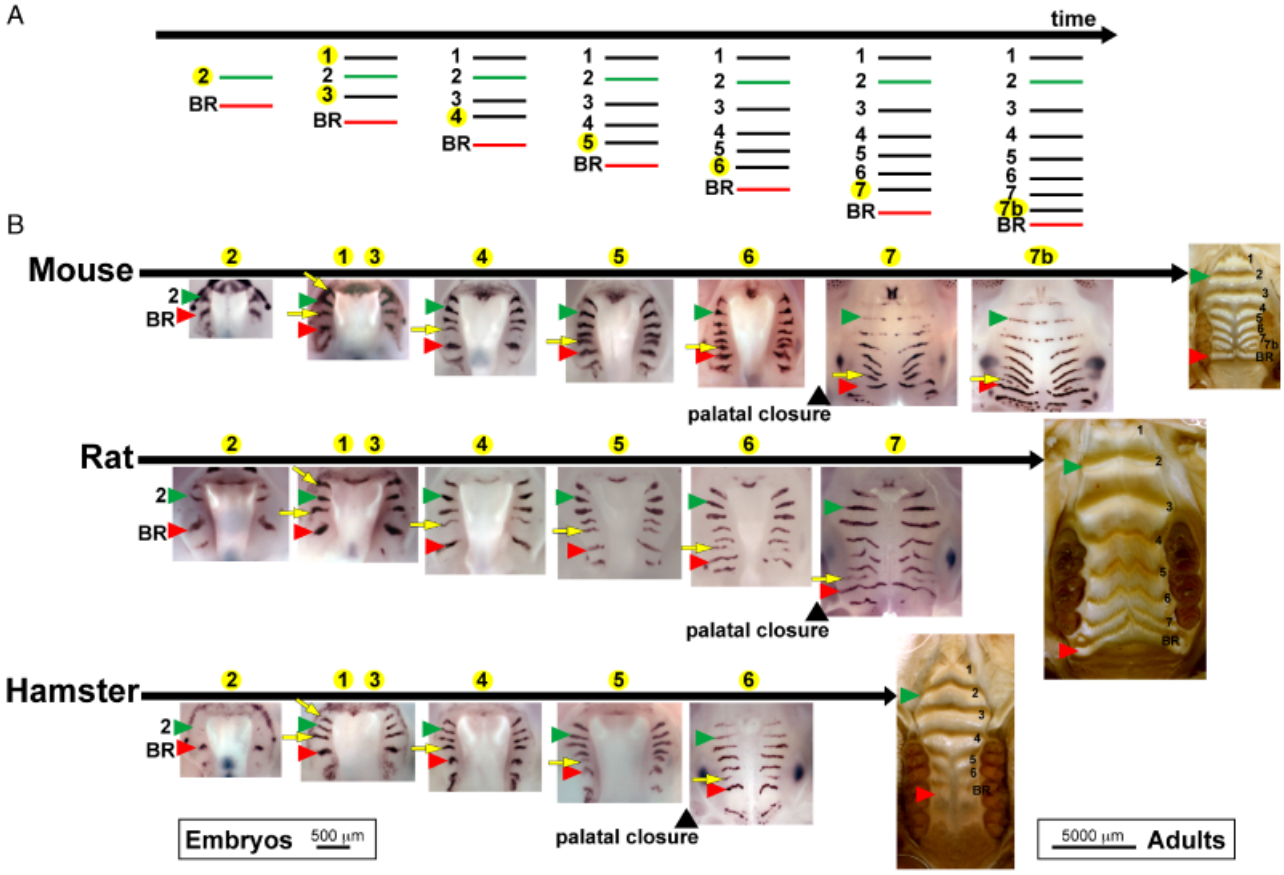

Fig. 2. Differences in rugae number between mouse, rat, and hamster are differences in the number of steps of the interposition process. (A) Scheme of the interposition process in mouse as previously shown in Pantalacci et al. 2008. Developmental time is schematized as a black arrow and rugae as small bars. The boundary ruga (BR) is the first one to form, followed by ruga 2. Rugae 3–7b are sequentially added in the growing region between ruga 2 and BR. At each step, the number of the latest formed ruga is highlighted. (B) Sequential addition of rugae between ruga 2 and the boundary ruga in mouse, rat, and hamster embryos. For each species, a series of embryonic palates is shown under a black arrow representing developmental time, with number of last formed rugae indicated on top of each picture (same scale for all embryo pictures, left bottom). Palates were hybridized with a species-specific *Shh* probe in order to visualize rugae. Note that palate is first open, and then closed upon palatal closure. Arrows point to the latest formed rugae and arrowheads point to ruga 2 and BR. Pictures showing the adult palate are also shown to the right (same scale for all adult pictures, right bottom).

Minor differences in rugae number between three muroid species (mouse, rat, hamster) are due to differences in the number of steps of the posterior interposition process

In a previous article (Pantalacci et al. 2008), we had deciphered the order of ruga formation in CD1 mice (Fig. 2A). We had shown that ruga 8, what we called the boundary ruga (BR), is formed first and is soon followed by ruga 2. Rugae 3–7b are then added sequentially between these two rugae, starting with ruga 3 and ending with ruga 7b. We had called this reiterative process "posterior interposition." Ruga 1 escapes this rule: it is added anterior to ruga 2. We also had shown that posterior interposition is at work in hamster, at least for rugae 4–6, ruga 6 being the BR.

We wondered whether the initial steps of rugae patterning in mouse might be conserved in rat and hamster, so that the difference in rugae number would then be due to a difference in number of steps of the interposition process. We thus obtained a full series of rat embryos (from days 14 to 17) and younger hamster embryos to complete the partial hamster series published previously (Pantalacci et al. 2008). As previously, we used whole mount in situ hybridization against the *Shh* gene to follow ruga formation. As in mouse, ruga 2 and BR formed first in both species, and posterior interposition then proceeds between these two rugae (Fig. 2B). Six steps are performed in mouse (adding ruga 3–7b), five in rat (ruga 3–7), and only four in hamster (ruga 3–6). Hence these three species differ in the number of steps of the interposition process.

Differences in rugae pattern are largely achieved during the posterior interposition process

The adult rugae pattern of mouse, rat, and hamster is shown on the right in Fig. 2B. They differ notably in terms of spacing between rugae and curvatures of rugae. We wondered whether these differences are mainly established during the course of the posterior interposition process and followed by mainly isometric growth, or whether allometric growth during the end of the fetal period or in the postnatal period could alter the pattern.

The curvature of rugae is not only species-specific but even ruga specific (see Fig. 2B). The fetal pattern at the end of the interposition process and the adult pattern are pretty much alike (Fig. 2B), suggesting that the curvature pattern is largely determined by the end of the process, and not deeply modified following it. Moreover, the specific curvature of each ruga might even be acquired during the formation of the ruga (see, e.g., formation of curved ruga 4 and 5 by comparison with more anterior rugae, in mouse, rat, and hamster on Fig. 2B).

The relative spacing of rugae can be quantified and compared between adults and fetus taken at the very end of the interposition process. For that purpose, we plotted the relative position of rugae for adult and fetal samples (i.e., the distance of each interposed ruga to ruga 2, divided by the distance between ruga 2 and BR, Fig. 3). In case of mouse, we treated hemipalates with and without 7b ruga separately. As shown in Fig. 3, the relative spacing pattern of rugae between ruga 2 and BR of fetuses strongly resembled that of adults (Fig. 3, see also Fig. 2B). Thus, in both adults and fetuses, spacing between rugae narrows posteriorly in mouse and rat, whereas in hamster it is more uniform. Relative distances between rugae thus seem to have been already largely determined at the end of the interposition process. For the three species however, we observed a trend to shift all rugae from rugae 4 slightly more posteriorly in adults. Thus, in future studies, the use of quantitative methods should help to evaluate departure from allometry (Klingenberg 1998) and shed light on post-interposition growth of the palate.

In conclusion, species differences in both ruga curvature and spacing pattern are largely achieved in the course of the interposition process, and the subsequent growth is largely isometric. We next investigated the differences in the interposition process during the development of these three species.

Two important prerequisites to comparative development: a precise staging of embryos and a comparison of developmental rates

In our previous article (Pantalacci et al. 2008), we proposed a simple model where ruga addition is only allowed at a minimal distance to the previous ruga and is coupled with mesiodistal growth of the region between ruga 2 and BR. In such a model, differences in three parameters may explain different final number of rugae between species: a difference in the minimal distance required to form a new ruga, a difference in the growth rate of the field between ruga 2 and BR, and finally a difference in the duration of the process.

In order to follow ruga addition and measure distances between rugae, whole mount in situ hybridization with an *Shh* probe as shown in Fig. 2 can be used. Of note, newly formed rugae have lower levels of *Shh* expression when compared with other rugae (e.g., rat ruga 7 or hamster ruga 6 in Fig. 2B), allowing us to distinguish slightly younger embryos, with a newly formed ruga, from slightly older embryos, with the next ruga ready to form. In these younger embryos, a measure of the distance between the newly formed ruga and its predecessor provides a proxy of the minimal distance required to form a new ruga.

Time is crucial to assess 2-BR growth rate and duration of the process, and we thus need a precise staging of embryos. Knowing only the number of days after detection of a vaginal plug is not sufficient. Indeed, time of coït and gestational conditions are sources of variability between litters, and even important intralitter developmental variability is commonly observed. Several studies have shown that embryo/fetus weight provides a reliable estimation of developmental stage (Wahlsten and Wainwright 1977; Peterka et al. 2002), and we thus established a statistical weight-to-time relationship for mouse, rat, and hamster (see "Materials and methods," Fig. S2 and also legend to Fig. S2 for further justification on using weight), which we then used to quantify embryo age from weight.

Once assessed, these parameters should be compared between species, and this requires to be aware of any difference in general developmental rate. Mouse and rat development are known to run in a parallel manner, with a delay of 1.5–2 days in rat due to later implantation (Altman 1962; Monie 1976). The golden hamster has one of the shortest gestation time among eutherian mammals (16 days, in comparison with 19 and 21 days, respectively, in mouse and rat) and this is known to be associated with late acceleration of developmental rates (Boyer 1948). We performed hamster–mouse and hamster–rat comparisons of development based on morphological criteria developed for mouse and rat by Theiler and Witschi, respectively (Fig. S3, Altman 1962; Theiler 1972). Between 9 and 12 days of development, hamster embryogenesis parallels that of mouse and rat, preceding mouse by approximately 1.5 day (Fig. S3). Later on, however, developmental rates are speeded up, and by 13 days of development, hamster embryos now precede mice by almost 2.5 days (Fig. S3). As a consequence, up to 12 days of development, hamster can be directly compared with mouse and rat, but the later period should be considered differently.

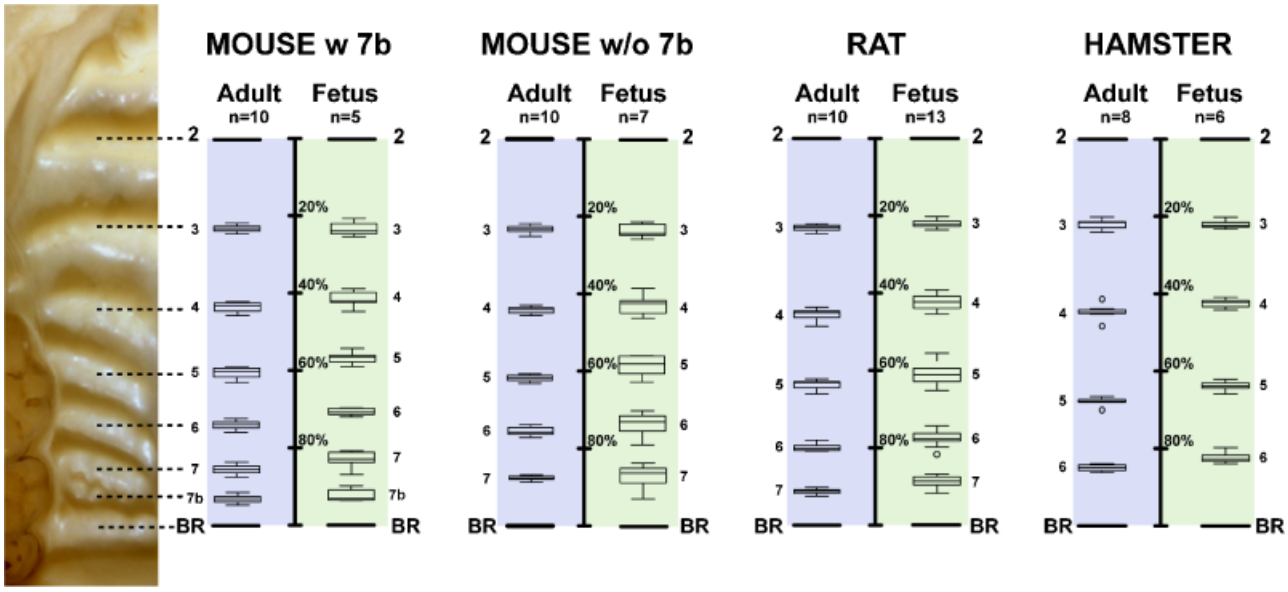

Fig. 3. Comparison of the adult ruga pattern with the fetal pattern at the end of the interposition process. For each case (mouse with [w] 7b, mouse without [w/o] 7b, rat, and hamster), a scheme allows comparison of the adult versus the fetal ruga pattern. The left part of the scheme represents the relative positions of rugae between ruga 2 (top, 0%) and ruga BR (bottom, 100%) in adults. For instance, in adult mouse, ruga 3 is found at approximately 22% of the 2-BR field. The right part of the scheme represents rugae relative position in fetus at the end of the interposition process. In case of mouse w/o 7b fetuses, only embryos as old as w 7b fetuses were taken, in order to make sure that they would never have developed a 7b ruga. The number (*n*) of hemi-palates measured is shown.

We now have sufficient tools and knowledge to measure and compare parameters of the interposition process in the three species.

Growth rate of the 2-BR field and median distance for addition of new rugae can differ between the three species, but the ratio between them is conserved

The mesio-distal growth of the field between ruga 2 and BR was almost linear in the three species (except for the last added ruga in mouse and rat), but rat had higher growth rates than both mouse and hamster, whose rates were similar (slope: 370 vs. 270 and 280 µm/day, respectively; Fig. 4A). Moreover, 2-BR length was higher in rat than in mouse and hamster all along the process. This is expected because rat embryos are bigger than mouse and hamster embryos of similar developmental stage.

We called d_{NEW} the distance between the penultimate and the latest formed rugae in embryos where *Shh* expression has just appeared (d_{NEW}, Fig. 4B). Within a species, d_{NEW} seems to slightly vary during the process, especially for the very last ruga (Fig. S4). Ruga 7b in mouse and ruga 7 in rat form at a significantly shorter distance than other rugae, while in hamster ruga 6 forms at a significantly higher distance than other rugae. When taken globally, the median d_{NEW} for all rugae is 114 µm in mouse, 157 µm in rat, and 120 µm in hamster (Fig. 4B). Thus mouse and hamster display similar values (differences are not significant), while rat displays a higher value (different from mouse and hamster with $P<0.001$), again in agreement with a larger embryo size.

In summary, the initial size of the 2-BR field at the beginning of the process, its growth rate and the median for d_{NEW} are similar in mouse and hamster, but higher in rat. This is in agreement with a size difference between mouse and hamster versus rat embryos from very early stages of embryogenesis. Interestingly, comparing the increase of 2-BR divided by median d_{NEW} gave a very similar picture for mouse and rat, both in terms of growth rate and ruga addition upon this growth (Fig. 4C). We concluded that the relationship between both the initial size and rate of growth of the 2-BR field and the median distance for formation of new rugae is roughly conserved in all three species, and that the difference in individual values seen between mouse and rat may mainly reflect a difference in overall size of these species.

A heterochronic shift in offset of the process (i.e., hypermorphosis) explains the one ruga difference between mouse and rat

Beside 2-BR growth rate and d_{NEW}, another source of variation in the final number of rugae may be in the onset or in the termination of the process. We have compared the timing of ruga interposition (Fig. 5 and Table S2) in the three species.

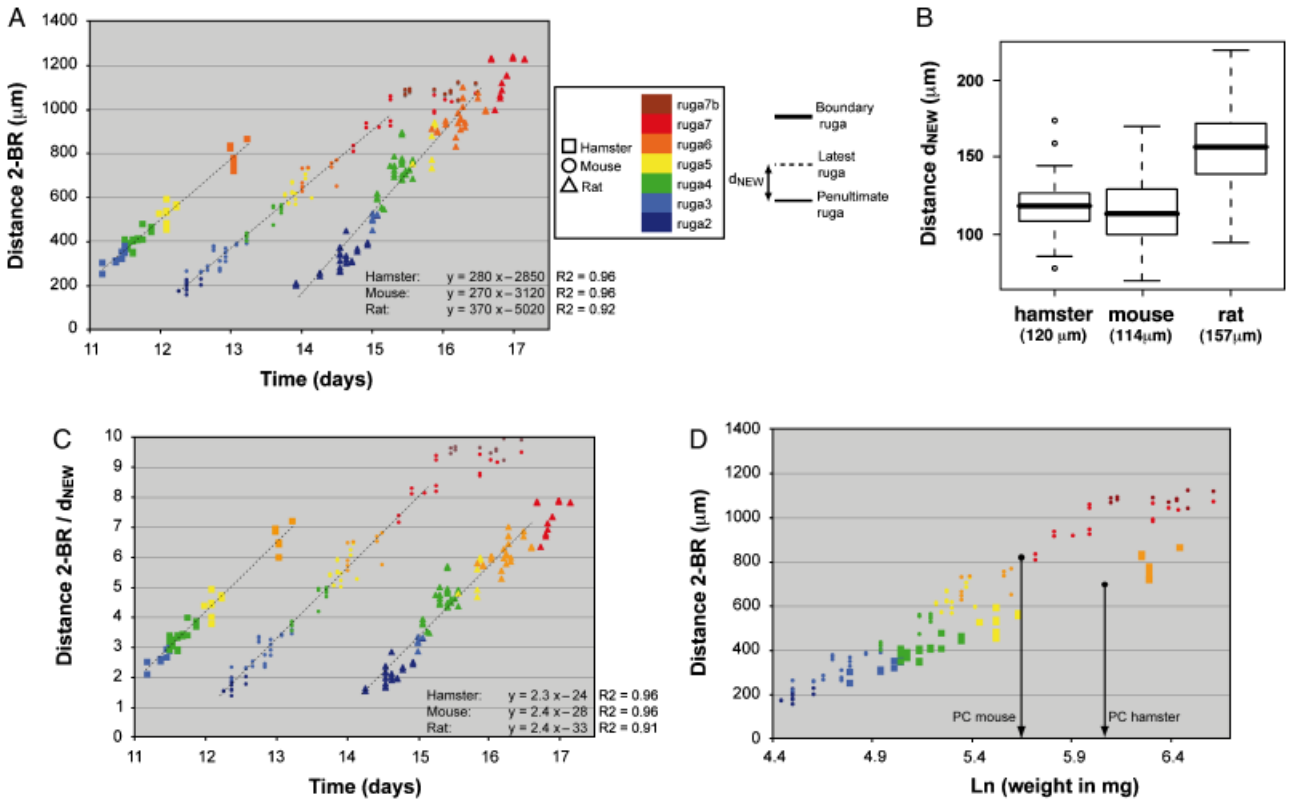

Fig. 4. Mesio-distal growth and distance for formation of new rugae during the interposition process in mouse, rat, and hamster embryos. (A) Mesio-distal growth of the field between ruga 2 and BR (in µm), depending on embryo age (in days) and species. The 2-BR distance was measured on *Shh*-hybridized embryos and the age of each embryo estimated from their weight. Colors represent the number of the latest added ruga in each embryo. Equations and R2 coefficients of linear regressions (not taking into account ruga 7b in mouse and ruga 7 in rat) are given at the lower right. (B) For each species, box plot showing the distance d_{NEW} between the latest and the penultimate formed ruga (in µm) in embryos of the three species. d_{NEW} was measured on *Shh* hybridized embryos, in which the latest ruga (i.e., ruga 3 up to ruga 7b) was added very recently, as judged from low-level *Shh* expression. Note that Fig. S4 details the values of d_{NEW} depending on the number of the latest formed ruga. The median d_{NEW} value is given in brackets for each species. (C) The same graph as in (A), except that the distance between ruga 2 and BR was divided by the species-specific median d_{NEW} value determined in (B). Equations and R2 coefficients of linear regressions (not taking into account ruga 7b in mouse and ruga 7 in rat) are given at the lower right. (D) Mesio-distal growth of the field between ruga 2 and BR, depending on ln of embryo weight for mouse and hamster; PC, palatal closure

For both mouse and rat, we could get embryos with newly formed ruga 2 and newly formed ruga 7 or 7b. As a consequence, we could roughly estimate the onset and the termination of the process, by using the median age of newly formed rugae 2 and the median age of newly formed rugae 7 (in mouse and rat) or rugae 7b (in mouse only) (Table S2). Remarkably, in both species formation of ruga 2, palatal closure and formation of ruga 7 occurred in a parallel manner, rat being delayed in each case by 1.6/1.7 days by comparison with mouse (the delay being, respectively, 1.6, 1.6, 1.7). This delay was moreover consistent with the already mentioned 1.5–2 days of delay of rat development by comparison with mouse. Thus, starting at a similar developmental stage, the process needed almost the same time to reach formation of ruga 7 in mouse and rat (mouse: 2.8 days; rat: 2.9 days), and, when forming, ruga 7b formed only later in mice (3.2 days).

In the meantime, however, there were differences in the dynamics of the process. Overall, the rhythm of ruga addition seemed more regular in rat than in mouse, and there was a clear difference in the beginning of the process: mouse tend to spend more time with only ruga 2, 3, and BR, whereas rat tend to spend more time with only ruga 2 and BR (compare embryo distributions for ruga 2 and 3 on Fig. 5). We concluded that despite some differences, especially in the timing of ruga 3 addition, the timing for ruga 2 and ruga 7 addition in rat was remarkably similar to that of mouse when considering the known developmental delay between these two species. This strongly suggested that addition of ruga 7b in mouse is due to a prolonged period of the interposition pro-

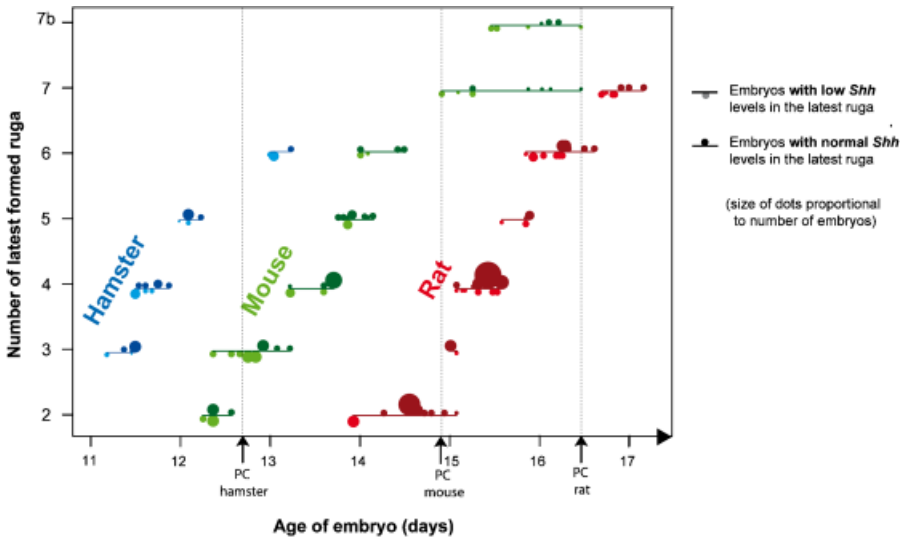

Fig. 5. Timing of rugae addition during mouse, rat and hamster development. For each species, the graphics show the relationship between embryo age (in days) and the step of the interposition process, in terms of number of the latest formed ruga (e.g., 2 means embryo with only ruga 2 and BR, 3 means embryo with ruga 2, 3 and BR, etc . . .). The line indicates the extent of the age distribution obtained for embryos at the same step. Age sampling is shown with dots whose size is proportional to the number of embryos with same age, and which sit under the line if the latest ruga is estimated to have formed very recently (according to low-*Shh* expression) or on top of the line if it is estimated to be older; PC, palatal closure.

cess in mouse relative to rat, that is a heterochronic phenomenon called hypermorphosis (Smith 2002).

In hamster, palatal growth rate does not follow the overall developmental acceleration associated with shortening of gestation, linking rugae number reduction to progenesis

As shown previously, up to 12 days of development, hamster embryogenesis parallels that of mouse, preceding it by approximately 1.5 days. This is precisely the time difference observed between mouse and hamster embryos with forming ruga 3 (Table S2; we were not able to get younger embryos with only ruga 2 and BR). Addition of ruga 4 and 5 also occurs during this period of parallel development, and might be slightly more rapid than in mouse (Table S2, Fig. 5).

In the next period, when hamster developmental rate is speeded up, palatal closure takes place and formation of ruga 6, instead of occurring before palatal closure like in mouse and rat, is strongly delayed and only occurs at day 13.0 (Fig. 5), that is at a developmental stage corresponding to formation of ruga 7 or even 7b in mouse (Fig. S3).

In conclusion, it seems that the interposition process in hamster starts at similar developmental stages as in mouse and first tends to be slightly more rapid than in mouse up to ruga 5 addition. However, upon strong acceleration of developmental rates, the process does not show any corresponding acceleration, and is in contrast severely delayed, ending at similar developmental stages as in mouse, with only addition of ruga 6. In agreement with this finding, the rate of 2-BR growth also shows no signs of acceleration (Fig. 4A). In this way, by comparison with the mouse, the length of the 2-BR field increases less rapidly than does the ln of embryo weight (Fig. 4D). As a consequence, the 2-BR field, which displays similar values as in mouse at the beginning of the process (around 300 μm, light blue dots for both species in Fig. 4A), is finally shorter upon palatal closure and at the end of the interposition process: it is only around 800 μm long upon ruga 6 addition in hamster but more than 900 and 1100 μm long upon ruga 7 and 7b addition, respectively, in mouse (compare hamster orange vs. mouse red and dark red dots in Fig. 4A). In conclusion, hamster palatal growth and the interposition process do not follow the speed up of overall maturation rate of the embryo (including palatal closure) occurring at the end of embryogenesis. The reduction of rugae number in hamster would thus be a typical case of progenesis, that is paedomorphosis by bringing forward the end of the patterning process (Smith 2002).

CONCLUDING REMARKS

We have shown that changes in rugae number by ± 1 are very frequent in muroid rodent evolutionary history. This is in line with the intuitive prediction that the repetitive nature of the interposition process responsible for adding new rugae between ruga 2 and BR should produce variations very easily. Comparison of development of three muroid species (among which hamster is distant to mouse and rat) confirmed that rugae number differences were indeed localized between ruga 2 and BR and associated with a different number of steps of the interposition process. Closer examination revealed that rugae number differences in these three species are due to heterochronies in the termination of the process. Indeed, we showed that adding a step in mouse is likely achieved by simply postponing the end of the process, while the loss of one step in hamster may be due to early termination of the process due to speed up of overall maturation and growth of embryo without any corresponding speed up in rates of palatal growth. The later case is probably very specific to the golden

hamster whose gestation time, the shortest known among eutherian mammals, is partly achieved by a sudden speed up of growth and maturation soon before the embryo to fetus transition (Boyer 1948). In comparison, the case of mouse versus rat might be quite typical of ± 1 changes seen in muroid rodent history. Together with a few other examples (see "Introduction"), our data illustrate how heterochronies explain meristic variation in traits that develop by sequential addition.

Moreover, we found that the ratio between mesio-distal palatal growth and the median distance for formation of new rugae is intriguingly similar in the three species. While we cannot rule out that this is simply by chance, it is tempting to suggest that this reflects developmental constraints on the evolution of the interposition process. Indeed, interposition seems to rely on lateral inhibition mechanisms coupled with growth (Pantalacci et al. 2008) and a precise balance between the two of them might be critical to robustness of the system.

Considering ruga evolution, an important question is the nature of internal constraints and selective pressures acting on rugae. In sensing and holding the food, their global pattern, in particular their spacing, is likely more important than their exact number. Because of the nature of the interposition process, "maintaining more or less similar spacing" could be somehow mechanically translated into "maintaining ± 1 rugae." In other words, ruga function may tolerate variations that could be imposed by other genetically or developmentally correlated traits (such as small variations in activation–inhibition parameters or variations in palatal length), and this could explain the observed relative stability of muroid ruga pattern with 8 ± 1 rugae. More drastic changes in rugae number are rare, yet possible because they are observed in two independent lineages (*Phloeomys*/*Uromys*, see Fig. 1). Interestingly these parallel drastic changes in rugae number show the same characteristics: antemolar rugae are preserved, as the very first intermolar rugae, and numerous small and close rugae are found more posteriorly. The same pattern was also observed by Eisentraut in two lineages of sciurid rodents (Eisentraut 1976). The evolutionary stability of the anterior rugae suggests either that they are inherently robust to variation due to internal constraints or that they are submitted to a stronger or at least different selective pressure. The later possibility is consistent with the fact that, in rodents, these rugae face a space without teeth (the diastema) and may this way play a special role in food processing. If this is true, then, if we think to the repetitive nature of ruga pattern formation, the necessity to maintain the anterior pattern may constrain the whole pattern. Indeed, whereas the "classical" patterns are consistent with almost the same parameters being repeatedly applied all along the process, patterns like the one seen in *Phloeomys* or *Uromys*, require that parameters like distance for ruga formation are more or less conserved for anterior rugae but change radically during the process for posterior rugae. There might be only a few ways to achieve uncouplings in a repetitive developmental mechanism; at least this is what suggested the study of another structure with sequential development. The neighboring molar row of muroid rodents also develops sequentially, starting with first molar and ending with third molar. Evolutionary speaking, the relative size between the three molars may be equal, or in a concerted gradient ($M1>>M2>M3$ or $M1<M2<<M3$), but only rarely independent (e.g., $M1<M2>M3$) (Kavanagh et al. 2007; Polly 2007). This suggests that achieving uncoupling of the steps of a sequential process is difficult, and may represent a general constraint to evolution of repeated structures. In the case of rugae, such a constraint, coupled with a strong selection pressure on anterior rugae, may take part in the conservative evolutionary pattern seen among muroid rodents.

Acknowledgments

We are grateful to J. Britton, F. Catzeflis, S. Renaud, and S. Reibel-Foisset for the loan of specimens and/or for pictures, and to Anne Lambert for technical help. We thank C. Lionnet for assistance at the PLATIM, and the PBES staff for animal care and breeding. We thank P. Weber and M. Paris for helpful discussion and L. McGowan for proofreading the manuscript. This work was supported by the Centre National pour la Recherche Scientifique (CNRS), the Ecole Normale Supérieure de Lyon and the ANR blanche program "Quenottes."

REFERENCES

Altman, P. L., and Dittmer, D. S. 1962. *Growth (including Reproduction and Morphological Development), Biological Handbooks*. Federation of American Societies for Experimental Biology, Washington, DC.

Boyer, C. C. 1948. Development of the golden hamster, *Cricetus auratus*, with special reference to the major circulatory channels. *J Morphol* 83: 1–38.

Eisentraut. 1976. Das Gaumenfaltenmuster der Säugetiere und seine Bedeutung für Stammesgeschichtliche und taxonomische Untersuchungen. In Zoologisches Forschunginstitut und Museum, A. Koenig Bonn (eds.). *Bonner Zoologische Monographien*. Eisentraut, Bonn, Germany, pp. 90–134.

Eisentraut. 1981. Ergänzende Untersuchungen am Gaumenfaltenmuster der Säugetiere. *Z. Säugetierkunde* 46: 79–89.

Galtier, N., Gouy, M., and Gautier, C. 1996. SEAVIEW and PHYLO_-WIN: two graphic tools for sequence alignment and molecular phylogeny. *Comput Appl Biosci* 12: 543–548.

Gomez, C., Ozbudak, E. M., Wunderlich, J., Baumann, D., Lewis, J., and Pourquie, O. 2008. Control of segment number in vertebrate embryos. *Nature* 454: 335–339.

Guindon, S., and Gascuel, O. 2003. A simple, fast, and accurate algorithm to estimate large phylogenies by maximum likelihood. *Syst Biol* 52: 696–704.

Halata, Z., Cooper, B. Y., Baumann, K. I., Schwegmann, C., and Friedman, R. M. 1999. Sensory nerve endings in the hard palate and papilla incisiva of the goat. *Exp Brain Res* 129: 218–228.

Hogan, B. L., Beddington, R. S., Costantini, F., and Lacy, E. 1994. *Techniques for Visualizing Gene Products, Cells, Tissues, and Organ Systems. Manipulating the Mouse Embryo, A Laboratory Manual*. Cold Spring Harbor Laboratory Press, Cold Spring Harbor, NY.

Huelsenbeck, J. P., and Ronquist, F. 2001. MRBAYES: bayesian inference of phylogenetic trees. *Bioinformatics* 17: 754–755.

Irvine, S. Q., Chaga, O., and Martindale, M. Q. 1999. Larval ontogenetic stages of Chaetopterus: developmental heterochrony in the evolution of chaetopterid polychaetes. *Biol Bull* 197: 319–331.
Ishizaki, K., Sakurai, K., Tazaki, M., and Inoue, T. 2006. Response of Merkel cells in the palatal rugae to the continuous mechanical stimulation by palatal plate. *Somatosens Mot Res* 23: 63–72.
Jansa, S. A., and Weksler, M. 2004. Phylogeny of muroid rodents: relationships within and among major lineages as determined by IRBP gene sequences. *Mol Phylogenet Evol* 31: 256–276.
Kavanagh, K. D., Evans, A. R., and Jernvall, J. 2007. Predicting evolutionary patterns of mammalian teeth from development. *Nature* 449: 427–432.
Klingenberg, C. P. 1998. Heterochrony and allometry: the analysis of evolutionary change in ontogeny. *Biol Rev Camb Philos Soc* 73: 79–123.
Lecompte, E., Aplin, K., Denys, C., Catzeflis, F., Chades, M., and Chevret, P. 2008. Phylogeny and biogeography of African Murinae based on mitochondrial and nuclear gene sequences, with a new tribal classification of the subfamily. *BMC Evol Biol* 8: 199.
Lecompte, E., Granjon, L., and Denys, C. 2002. The phylogeny of the Praomys complex (Rodentia: Muridae) and its phylogeographic implications. *J Zoolog Syst Evol Res* 40: 8–25.
Lee, C. S., Nishida, T., and Mochizuki, K. 1975. Normal prenatal growth of the golden hamster (author's transl). *Jikken Dobutsu* 24: 53–60.
McNamara, K. J. 1997. *Shapes of Time: Evolution of Growth and Development*. Johns Hopkins University Press, Baltimore, MD.
Monie, I. W. 1976. Comparative development of the nervous, respiratory, and cardiovascular systems. *Environ Health Perspect* 18: 55–60.
Nunzi, M. G., Pisarek, A., and Mugnaini, E. 2004. Merkel cells, corpuscular nerve endings and free nerve endings in the mouse palatine mucosa express three subtypes of vesicular glutamate transporters. *J Neurocytol* 33: 359–376.
Pagel, M., Meade, A., and Barker, D. 2004. Bayesian estimation of ancestral character states on phylogenies. *Syst Biol* 53: 673–684.
Pantalacci, S., et al. 2008. Patterning of palatal rugae through sequential addition reveals an anterior–posterior boundary in palatal development. *BMC Dev Biol* 8: 116.
Peterka, M., Lesot, H., and Peterkova, R. 2002. Body weight in mouse embryos specifies staging of tooth development. *Connect Tissue Res* 43: 186–190.
Polly, P. D. 2007. Evolutionary biology: development with a bite. *Nature* 449: 413–415.
Posada, D., and Crandall, K. A. 1998. MODELTEST: testing the model of DNA substitution. *Bioinformatics* 14: 817–818.
Poux, C., and Douzery, E. J. 2004. Primate phylogeny, evolutionary rate variations, and divergence times: a contribution from the nuclear gene IRBP. *Am J Phys Anthropol* 124: 1–16.
Raff, R. A. 1996. *The Shape of Life: Genes, Development, and the Evolution of Animal Form*. University of Chicago Press, Chicago.
Raff, R. A., and Wray, G. A. 1989. Heterochrony—developmental mechanisms and evolutionary results. *J Evol Biol* 2: 409–434.
Richardson, M. K., and Oelschlager, H. H. 2002. Time, pattern, and heterochrony: a study of hyperphalangy in the dolphin embryo flipper. *Evol Dev* 4: 435–444.
Shapiro, M. D., Hanken, J., and Rosenthal, N. 2003. Developmental basis of evolutionary digit loss in the Australian lizard Hemiergis. *J Exp Zoolog B Mol Dev Evol* 297: 48–56.
Smith, K. K. 2002. Sequence heterochrony and the evolution of development. *J Morphol* 252: 82–97.
Smith, K. K. 2003. Time's arrow: heterochrony and the evolution of development. *Int J Dev Biol* 47: 613–621.
Steppan, S., Adkins, R., and Anderson, J. 2004. Phylogeny and divergence-date estimates of rapid radiations in muroid rodents based on multiple nuclear genes. *Syst Biol* 53: 533–553.
Team, R. D. C. 2008. *R: A Language and Environment for Statistical Computing*. R. F. f. S. Computing, Vienna, Austria.
Theiler. 1972. *The House Mouse*. Springer-Verlag, Berlin.
Wahlsten, D., and Wainwright, P. 1977. Application of a morphological time scale to hereditary differences in prenatal mouse development. *J Embryol Exp Morphol* 42: 79–92.

SUPPORTING INFORMATION

Additional supporting information may be found in the online version of this article:

Table S1. Material for reconstruction of rugae number history in muroid rodents. Excel sheet with for each taxa number of rugae with references and accession number of sequences used for phylogenetic reconstruction.

Table S2. Addition time of the different rugae and duration of the process during mouse, rat and hamster development. The left part of the table provides the median age of embryos at each step of the interposition process, from addition of ruga 2 up to addition of ruga 7b. Age for palatal closure is provided, with number of days since median age for ruga 2 addition in brackets. The right part of the table provides the duration between addition of two particular rugae (as the difference between the median age of the corresponding stages).

All these values are provided for samples with a very recently formed ruga (low *Shh* expression) or for all samples. Distributions of corresponding samples is shown on Fig. 5.

Figure S1. Maximum likelihood tree for the combined dataset. A black dot indicates that $BP_{ML} \leq 95$ and $PP = 1.0$. Otherwise values are indicated as follow: PP/BP_{ML}. An " – " indicates that MrBayes or Phyml boostrap analysis supports an alternative topology.

Figure S2. Weight-to-time relationship for the three species. Despite it is used widely in developmental studies, age determined according to detection of vaginal plug after overnight mating of rodents only provides a rough estimates of developmental time ($\pm$ 0.5 days difference in mouse (Peterka et al. 2002), to be compared with the 3 days needed to achieve the whole ruga pattern). Moreover, intra-litter variations also can rise up to 0.5 days differences (Peterka et al. 2002). We recorded this age for our embryos series, but it was clearly not reliable enough for the precision we wanted to achieve.

Three other methods have been put forward, at least for mouse embryos, based on: (i) body weight (ii) crown-rump length measurement (iii) morphological criteriae: Theiler staging is classically used, but does not allow precise staging. Whalsten and Wainwright (Wahlsten and Wainwright 1977) developed a scoring method for mouse embryo staging where features in 4 external organs (skin, limb, eye and ear) are scored and morphological age is obtained as an average score of the four of them.

Importantly, all three methods have been shown to be highly correlated *"Morphological age for an embryo or fetus is shown to correlate highly with ages estimated from body weight and crown-rump length"* (Wahlsten and Wainwright 1977). Among them, we chose embryo weighting as it is the most practical, and in particular, it allows rapid and minimal handling of embryos, which is important for preserving RNA for

in situ hybridization. It is reliable enough to allow following development of highly dynamic developing structures like tooth buds (Peterka et al. 2002) but also rugae (Pantalacci et al. 2008). Lastly, this method could be used for the three species (whereas precise scoring methods such as the one described for mouse have not been described for mouse and rat to our knowledge).

The curves represented in this figure are standardization curves (age/weight) obtained from a high number of embryos (and litters) for which weight and a rough age were known (according to detection of vaginal plug). For each species, age of embryos was plotted against embryo weight and a logarithmic relationship (shown in red) was deduced for a time period including the time period of interest in this study. For hamster, our data (in red) fitted with published data (in black, Lee et al. 1975), except for two litters for which coït time was obviously misestimated (see methods for details).

Figure S3. comparison of hamster developmental rate with these of mouse and rat. Two by two comparisons of developmental stages (hamster-rat, according to Witschi stages; hamster-mouse, according to Theiler stages) were made based on (Boyer 1948; Altman 1962; Theiler 1972). They are summarized in the table (A), which gives the days of development in each species for similar developmental stages, and represented in the graph (B) including the period of interest in this study.

Figure S4. Minimal distance for formation of new rugae, as evaluated from the distance between the penultimate and the latest formed ruga, and depending on rugae number of mouse, rat and hamster embryos. Graphs show for each latest formed ruga the distance between him and the penultimate formed ruga (in micrometers) as measured on *Shh* hybridized embryos of the three species (n = number of embryos measured in each case). The data are presented for embryos in which the latest ruga was added very recently (as judged from low-level *Shh* expression, d_{NEW}) and for all sampled embryos (regarding less of *Shh* expression level, d), showing that the tendencies are similar despite the low number of embryos represented in some cases for d_{NEW}. d_{NEW} and d are not constant throughout the process of ruga addition (the effect of the number of rugae is significant according to ANOVA tests, whose *P*-values are presented for each plot in the left upper corner). We tested individually the effect of number of rugae by contrasting one particular ruga *versus* all the others (the *P*-values of the corresponding ANOVA are represented by stars above each box-plot when significant: $^{*}0.001 < P\text{-value} < 0.05$; $^{**}P\text{-value} < 0.001$).

Please note: Wiley-Blackwell are not responsible for the content or functionality of any supporting materials supplied by the authors. Any queries (other than missing material) should be directed to the corresponding author for the article.